Copy No.

NACA

RESEARCH MEMORANDUM

STABILITY AND CONTROL CHARACTERISTICS OF A FREE-FLYING MODEL

WITH AN UNSWEPT WING OF ASPECT RATIO 3 (XS-3)

By

Charles V. Bennett and James L. Hassell, Jr.

Langley Aeronautical Laboratory
Langley Field, Va.

NATIONAL ADVISORY COMMITTEE
FOR AERONAUTICS
WASHINGTON

NACA RM No. L8J04

RESEARCH MEMORANDUM

STABILITY AND CONTROL CHARACTERISTICS OF A FREE-FLYING MODEL

WITH AN UNSWEPT WING OF ASPECT RATIO 3 (XS-3)

By Charles V. Bennett and James L. Hassell, Jr.

SUMMARY

An investigation of the low-speed flying characteristics of a low-aspect-ratio airplane configuration has been conducted in the Langley free-flight tunnel. The model consisted of a thin unswept wing of aspect ratio 3 mounted on a circular fuselage of fineness ratio 9.33 to simulate the XS-3 research airplane.

The results of the tests indicated that the static longitudinal stability characteristics of the model with flaps retracted were satisfactory. With the flaps deflected the longitudinal stability decreased with increasing lift coefficient so that it was necessary to move the center of gravity to the leading edge of the mean aerodynamic chord to obtain stability at the stall. The longitudinal stability could be increased over the lift range by moving the horizontal tail upward, but the variation of stability with lift coefficient for the flaps-deflected configuration was not eliminated. The dynamic longitudinal stability characteristics of the model were satisfactory when sufficient static stability was provided.

The model had high static directional stability over the entire lift range. The dynamic lateral stability characteristics of the model were satisfactory at all lift coefficients up to the stall, but because of the small span of the aspect ratio 3 model the rolling motions were faster and more difficult to control than those for models of higher aspect ratio. At the stall, erratic rolling motions were encountered which were very difficult to control. The lateral-flight characteristics were considered unsatisfactory when the directional-stability factor C_{n_β} was less than 0.002 because large yaw angles were reached which caused difficulty in maintaining control. A larger value of C_{n_β} was required for satisfactory flying characteristics for the aspect ratio 3 model than is required for models of higher aspect ratio.

INTRODUCTION

The use of low-aspect-ratio wings has been proposed as a possible means of eliminating or minimizing some of the problems of high-speed flight. As a part of a general research study of the stability characteristics of low-aspect-ratio wings, an investigation was conducted in the Langley free-flight tunnel to determine the low-speed stability and control characteristics of an airplane model with an unswept aspect ratio 2 wing (reference 1). This work showed that the flight characteristics of the aspect ratio 2 model were not as good as those of an aspect ratio 6 model. The present investigation was undertaken in order to obtain data for an intermediate aspect-ratio model and to determine the low-speed flight characteristics of a model similar to the XS-3 airplane, a high-speed airplane configuration equipped with a thin unswept wing of aspect ratio 3 and taper ratio 0.4.

The investigation included force and flight tests of a model with an unswept aspect ratio 3 wing and a fuselage of fineness ratio 9.33. Tests were made with flaps retracted and extended. In addition, the effect on flight characteristics of mass distribution, horizontal-tail location, and static directional stability was obtained. Calculations were made to determine the oscillatory-stability boundaries of the test model and the results of these calculations were correlated with the flight results.

SYMBOLS

The forces and moments were measured about the stability axes. A diagram of these axes showing the positive directions of the forces and moments is given as figure 1.

α — angle of attack, degrees

C_L — lift coefficient (Lift/qS)

C_D — drag coefficient (Drag/qS)

C_m — pitching-moment coefficient (Pitching moment/$qS\bar{c}$)

C_l — rolling-moment coefficient (Rolling moment/qSb)

C_n — yawing-moment coefficient (Yawing moment/qSb)

C_Y — lateral-force coefficient (Lateral force/qS)

S   wing area, square feet

$\dot{q}$ dynamic pressure, pounds per square foot

b   wing span, feet

V   airspeed, feet per second

k_{X_0} radius of gyration about the principal X-axis, feet

k_{Z_0} radius of gyration about the principal Z-axis, feet

γ flight-path angle, positive refers to climb, degrees

η angle of attack of principal longitudinal axis of airplane, positive when principal axis is above flight path at the nose, degrees

W   weight, pounds

W/S   wing loading, pounds per square foot

l tail length, measured from center of gravity to center of pressure of tail, feet

$\bar{c}$ mean aerodynamic chord, measured in plane parallel to plane of symmetry, feet $\left(\dfrac{2}{S}\displaystyle\int_0^{b/2} c^2 \, db\right)$

ρ mass density of air at standard conditions, slugs per cubic foot

β angle of sideslip, degrees

$\dfrac{rb}{2V}$ yawing-angular-velocity parameter, radians

$\dfrac{pb}{2V}$ helix angle generated by wing tip (rolling-angular-velocity parameter), radians

μ relative-density factor $(m/\rho Sb)$

m   mass, slugs

C_{l_β} effective-dihedral parameter; rate of change of rolling-moment coefficient with angle of sideslip, per degree $\left(\dfrac{\partial C_l}{\partial \beta}\right)$

C_{n_β} directional-stability parameter; rate of change of yawing-moment coefficient with angle of sideslip, per degree unless otherwise noted $\left(\dfrac{\partial C_n}{\partial \beta}\right)$

C_{Y_β} effective side-area parameter; rate of change of lateral-force coefficient with angle of sideslip, per degree unless otherwise noted $\left(\dfrac{\partial C_Y}{\partial \beta}\right)$

C_{n_p} rate of change of yawing-moment coefficient with rolling-angular-velocity factor, per radian $\left(\dfrac{\partial C_n}{\partial \frac{pb}{2V}}\right)$

C_{l_p} rate of change of rolling-moment coefficient with rolling-angular-velocity factor, per radian $\left(\dfrac{\partial C_l}{\partial \frac{pb}{2V}}\right)$

C_{Y_p} rate of change of lateral-force coefficient with rolling-angular-velocity factor, per radian $\left(\dfrac{\partial C_Y}{\partial \frac{pb}{2V}}\right)$

C_{n_r} rate of change of yawing-moment coefficient with yawing-angular-velocity factor, per radian $\left(\dfrac{\partial C_n}{\partial \frac{rb}{2V}}\right)$

C_{l_r} rate of change of rolling-moment coefficient with yawing-angular-velocity factor, per radian $\left(\dfrac{\partial C_l}{\partial \frac{rb}{2V}}\right)$

C_{Y_r} rate of change of lateral-force coefficient with yawing-angular-velocity factor, per radian $\left(\dfrac{\partial C_Y}{\partial \frac{rb}{2V}}\right)$

i incidence, degrees

5

R   Routh's discriminant $(R = BCD - AD^2 - B^2E = 0)$

where

A, B, C, D, and E are coefficients of the stability equation

Subscripts:

t   horizontal tail

w   wing

APPARATUS

The investigation was conducted in the Langley free-flight tunnel, which is designed to test free-flying dynamic models. A complete description of the tunnel and its operation is given in reference 2. The force tests were made on the free-flight-tunnel six-component balance which is described in reference 3. This balance rotates in yaw with the model so that all forces and moments are measured about the stability axes shown in figure 1.

Photographs of the model, used to simulate the XS-3 airplane, are shown in figure 2 and a three-view sketch is shown in figure 3. The model was a midwing configuration and had a circular section fuselage of fineness ratio 9.33, the aft portion of which was blunt. The conventional stabilizing surfaces were mounted on a boom aft and above the fuselage. The unswept double-wedge airfoil section of aspect ratio 3 and taper ratio 0.4 was equipped with full-span 0.15-chord leading-edge flaps which were deflected 0° or 30° and inboard trailing-edge split flaps of 0.30 chord which deflected 0° or 60°. The flap-deflected configuration consisted of the trailing and leading-edge flaps deflected simultaneously.

The model was so constructed that the horizontal-tail incidence, the vertical location of the horizontal tail, and the mass distribution could be varied. The directional stability of the model could also be varied by mounting vertical fins of various sizes along the fuselage both ahead of and behind the center of gravity.

The dimensional and mass characteristics of the model are shown in table I.

TESTS AND CALCULATIONS

Force Tests

Force tests were made over an angle-of-attack range from 0° to 20° to determine the static longitudinal stability characteristics of the model with flaps retracted and deflected for two vertical locations of the horizontal stabilizer. The incidence of the stabilizer was varied from 0° to -10°.

Tests to determine the static lateral stability characteristics of the model with flaps retracted and deflected and with the vertical tail off and on were made at $\psi = \pm 5°$ over an angle-of-attack range from 0° to 20°. In addition, data were obtained with various amounts of directional stability by mounting vertical fins of different sizes along the fuselage both ahead of and behind the center of gravity as shown in table II. Aileron-effectiveness tests were made with the left aileron deflected ±6° and ±12° over an angle-of-attack range from 0° to 20°.

All force tests were made at a dynamic pressure of 3.0 pounds per square foot which corresponds to a test Reynolds number of approximately 250,000 based on the mean aerodynamic chord of 0.785 foot.

Rotation Tests

Values of C_{n_p} and C_{l_p} for the model wing were obtained by the forced rotation method in the Langley 20-foot free-spinning tunnel. For these tests, the model wing was mounted on a rotating strut in the vertical air stream, and yawing and rolling moments were measured for two rates of rolling rotation.

Flight Tests

Flight tests to determine the dynamic longitudinal and lateral stability characteristics were made with the center-of-gravity position varied from 0 to 10 percent of the mean aerodynamic chord. The lightly loaded model was flown over a lift-coefficient range from 0.42 to 0.62 with flaps retracted and from 0.47 to 1.17 with the flaps deflected. Addtional flight tests were made with the flaps deflected, with the model heavily loaded, over a lift-coefficient range from 0.47 to 1.04. The mass characteristics for the light and heavy loading conditions are given in table I. In addition, flight tests were made to determine the effect upon the lateral flight behavior of decreasing the

directional stability by decreasing the size of the vertical tail or by adding vertical fin area forward of the center of gravity. (See table II.)

Calculations

Calculations were made by the method of reference 4 to determine the boundary of zero damping of the lateral oscillations (R = 0) for a lift coefficient of 0.6 for the flap-retracted configuration and for lift coefficients of 0.70 and 1.0 for the flap-extended configuration. The aerodynamic, geometric, and mass characteristics used in the calculations are presented in table III. The mass characteristics of the model were obtained by measurement; and flight-path angle, trim airspeed, and angle of attack for each lift coefficient were obtained from flight tests. The values of $C_{Y_\beta (tail\ off)}$ and $C_{n_\beta (tail\ off)}$ were obtained from force tests. The values of $C_{n_p (tail\ off)}$ were calculated by the equation of reference 5

$$C_{n_p} = \frac{-\left(C_L - \dfrac{dC_{D_W}}{d\alpha}\right)}{8}$$

which has been verified by unpublished experimental data. The other tail-off stability parameters were estimated from the charts of reference 6. The tail contributions to these parameters were calculated by equations similar to those of reference 7.

RESULTS AND DISCUSSION

Force Tests

Longitudinal stability.- The static longitudinal stability characteristics of the model are shown in figures 4 to 8. The data of figure 4 show the effect of flap deflection on the lift, drag, and pitching-moment characteristics of the model for the basic configuration with the center of gravity at the leading edge of the mean aerodynamic chord. These data show that deflecting the flaps increased the lift coefficient at which the lift curve broke (considered herein to be the maximum lift coefficient) from 0.64 to 1.19. These data also indicate that with the flaps retracted the model had satisfactory longitudinal stability characteristics over the linear portion of the lift curve

after which there was a slight nosing-up tendency. The flap-extended data of figure 4 indicate a decrease in the static longitudinal stability over the lift range such that for the center-of-gravity location at the leading edge of the mean aerodynamic chord, neutral stability was obtained before maximum lift was reached. The stability was increased for the flap-retracted and flap-deflected configurations when the incidence of the horizontal tail was changed from 0° to -5° or -10° as shown in figures 5 and 6.

In an attempt to improve the static longitudinal stability characteristics at the higher lift coefficients, the horizontal tail was moved upward 4 inches on the vertical tail; and the results for this configuration are presented in figures 7 and 8 for the flap-retracted and flap-extended configurations, respectively. The flap-retracted data of figure 7 indicate that with the high horizontal-tail location the static margin was increased by about 0.10 over the linear portion of the lift curve. The instability that was noted for the lower horizontal-tail location was not eliminated but was delayed approximately 2° by the upward movement of the horizontal tail.

The flap-extended data of figure 8 show that the upward movement of the horizontal tail resulted in an increase in stability over the lift range of about 0.12 static margin.

Lateral stability.- The effect of flap deflection on the lateral stability characteristics is shown in figure 9. These data indicate that a relatively high degree of directional stability $\left(C_{n_\beta} \text{ over } 0.005\right)$ was obtained with the flaps retracted up to the angle of attack for maximum lift coefficient $(\alpha = 12^\circ)$. After the angle of attack for maximum lift coefficient was reached, the directional stability was reduced somewhat but was still relatively high. The flap-deflected data indicate the directional stability was increased by flap deflection over the entire angle-of-attack range even after the angle of attack for maximum lift. The effective dihedral is positive $\left(-C_{l_\beta}\right)$ and large over the angle-of-attack range for both the flap-retracted and flap-deflected configurations.

Flight Tests

Flaps retracted.- The dynamic longitudinal stability characteristics with the flaps retracted were satisfactory throughout the lift-coefficient range tested (0.42 to 0.62) with the center of gravity at the leading edge of the mean aerodynamic chord. The longitudinal instability indicated in figure 4 for 0° incidence was not experienced in flight because with the center-of-gravity location used it was necessary to use the -10° stabilizer incidence for trim at the stall and this tail incidence provided stability at the stall

as shown in figure 5. It appeared in the tests that when satisfactory static longitudinal stability was provided, the dynamic longitudinal stability characteristics were satisfactory.

The flap-retracted flight tests to determine the dynamic lateral stability characteristics indicated that flights could be made with no difficulty with the ailerons alone or with the ailerons and rudder interconnected at angles of attack below the angle of maximum lift ($\alpha = 12^\circ$). However, the rolling motions were much faster for the aspect ratio 3 wing model used in the present investigation than for the aspect ratio 6 model investigation which was reported in reference 1. The ease with which the model could be flown with ailerons alone was attributed to the small adverse yawing motions. These motions were small because of the large amount of static directional stability (fig. 9), the low adverse yaw due to aileron deflection as shown in figure 10, and the positive value of the yawing moment due to rolling factor C_{n_p} for this wing which is shown in figure 11.

In reference 1 it was found that the adverse yaw due to aileron deflection increased as the aspect ratio of the wing was decreased. The wing used in the present investigation, however, does not show this trend when compared with the data for wings of aspect ratios 6 and 2 from reference 1. (See fig. 10.) Instead, the aspect ratio 3 wing has much smaller adverse aileron yawing moments than either the aspect ratio 6 or 2 wings. This difference is believed to be caused by the fact that the aspect ratio 3 wing has a very thin section with a sharp leading edge, whereas the wings of reference 1 had conventional round-nose airfoil sections.

The positive C_{n_p} of the aspect ratio 3 wing used in the present investigation is compared with similar unpublished data for a highly cambered round-nose wing of identical plan form in figure 11. These data show that the present wing has positive C_{n_p} whereas the cambered section has negative C_{n_p}. This difference is in agreement with the values of C_{n_p} that were calculated by the equation for C_{n_p} given in reference 5.

In the flap-retracted flight tests made at lift coefficients which corresponded to angles of attack above 12° (after break in lift curve), erratic rolling motions were encountered and the model appeared to have very little damping in roll. This result is verified by the rotation-test data of figure 11 which show that the damping-in-roll factor C_{l_p} dropped to zero at 16° angle of attack. The aileron control was powerful enough but because of the relatively high rolling velocities of this small-span model, the pilot had considerable difficulty in

applying lateral control to keep the model flying smoothly at these angles of attack. At times, the pilot inadvertently reinforced the erratic rolling motions, particularly in flights with the heavy loading condition in which the increased rolling inertia caused "overshooting" in controlling the attitude of the model in roll.

There was no sign of oscillatory instability in any of the flights made with the flaps retracted. The location of the oscillatory stability boundary as shown by figure 12 indicates that the lateral oscillation would be stable for any positive value of directional stability. This boundary is valid only for a lift coefficient of 0.6, however, and would be expected to shift upward with decreasing lift coefficient. The most critical lateral-stability condition with flaps retracted would probably be at very high speeds which could not be simulated in the Langley free-flight tunnel.

Flaps deflected.- Flight tests made with the flaps deflected indicated that the dynamic longitudinal stability was satisfactory below a lift coefficient of 0.65 with the center of gravity at 0.10 mean aerodynamic chord. At lift coefficients above 0.65, the longitudinal stability decreased, and constant attention to the elevator control was required to prevent the model from nosing up. The force-test data of figure 13 show the decreased stability at high lift coefficients for this center-of-gravity position. The pitching motions were not of a particularly violent nature because the nosing-up tendency was rather mild. When the center of gravity was moved to 0.05 mean aerodynamic chord the longitudinal stability was satisfactory up to a lift coefficient of 0.80. When the lift coefficient was increased above 0.65 for the 0.10 mean aerodynamic chord center-of-gravity position or 0.80 for the 0.05 mean aerodynamic chord center-of-gravity position, the longitudinal stability became progressively worse and the model usually nosed up, stalled, rolled off, and crashed.

With the center of gravity located at the leading edge of the mean aerodynamic chord, the model could be flown up to a lift coefficient of 1.17 with no difficulty. As in the case of flaps retracted the negative tail incidence required for trim at the stall had a stabilizing effect on the pitching-moment curve at the stall, and this effect plus the stabilizing effect of moving the center of gravity forward accounted for the ability to fly the model up to a higher lift coefficient with the center of gravity at the leading edge of the mean aerodynamic chord.

Flights made with the horizontal tail moved upward 4 inches and with the center of gravity at 0.05 mean aerodynamic chord indicated that the model could be flown up to a lift coefficient of 1.05 compared with a lift coefficient of 0.80 with the lower horizontal-tail location. Above a lift coefficient of 1.05 the model tended to nose-up but could usually be controlled fairly well with the elevator. The improved

flying characteristics with the high position of the horizontal tail
would be expected from the force-test data of figure 8 which show
that the static stability was increased over the entire lift range
and that a higher angle of attack was reached before static
instability occurred.

Lateral-flight characteristics of the model with flaps deflected
were considered satisfactory over a lift-coefficient range from 0.47
to 1.17. These flights were made with the light condition and with
the center of gravity at the leading edge of the mean aerodynamic
chord. As the model stalled, there was a slight rolling tendency,
but the dropping wing could usually be picked up by the ailerons which
retained some effectiveness at the stall. Flights made with the heavy
loading at lift coefficients from 0.57 to 1.1 indicated that the flight
characteristics were slightly worse than for the light-loading
condition because the increased inertia resulted in an overshooting
tendency similar to that previously described for the flaps-retracted
condition.

Effect of directional stability.- The results of the flights to
determine the effect of decreasing the directional stability are
summarized in figure 14. The vertical-tail configurations tested are
shown on table II along with the values of C_{n_β}, C_{l_β}, and C_{Y_β} that
were determined from force tests. The values of C_{n_r} were estimated
from the equation

$$C_{n_r} = C_{n_r(tail\ off)} - 2\frac{l}{b}C_{n_\beta(tail)}$$

The value of C_{n_r} for the tail-off condition was calculated by
assuming that the tail boom acted as a vertical tail with the tail
length measured to the center of area of the boom. The large value
of C_{n_β} of the tail boom accounts for the large value of C_{n_r} that
was obtained with the tail off. All of these flights were made at a
lift coefficient of approximately 0.7.

The results of the tests in which the directional stability was
decreased by removing vertical-tail area showed that the model could
be flown with no difficulty when the directional-stability factor C_{n_β}
was reduced from 0.0085 to 0.0064. When C_{n_β} was decreased to 0.0019,
the model yawed considerably but did not get out of control even with
the ailerons alone. A further decrease in C_{n_β} to 0.0014 resulted
in increased yawing motions but the model could still be flown ailerons

alone. Crashes were frequent with this condition, however, because of the large yawing motions. These results indicate that the present model could be flown satisfactorily with values of C_{n_β} lower than the minimum values that were considered satisfactory for the aspect ratio 2 wing which was reported in reference 1. It is believed that the smaller adverse yawing moments of the aspect ratio 3 model probably caused this difference in flight characteristics. No flights were made with the ailerons and rudder interconnected for values of C_{n_β} below 0.0064 because removal of both the fin and rudder was necessary to reduce C_{n_β} to 0.0019.

The flight tests made with the directional stability reduced by adding vertical-fin area ahead of the center of gravity (so that rudder control could be maintained) show that the model could be flown with the directional stability as low as 0.0023 with ailerons and rudder interconnected or with ailerons alone. Below 0.0023 the model tended to fly in a slipped attitude after a disturbance and could not be corrected by the ailerons. This condition was not unlike those reported in reference 8 in which a model was considered unsatisfactory with a combination of low directional stability and high values of the lateral-force parameter C_{Y_β}. High values of C_{Y_β} were obtained in the present tests when large lateral areas were used.

The high values of the damping-in-yaw parameter C_{n_r} which also were obtained with these vertical-fin configurations (table II) tended to oppose the yawing motions; but once the model reached a large yaw angle, the damping also tended to resist the return to zero yaw. This damping-in-yaw effect was studied in detail in the investigation reported in reference 9. It is of interest to note, however, that the values of C_{n_r} obtained in the present investigation were from 2 to 10 times as large as the largest used in reference 9. The relatively large values of C_{n_r} for the present model can be explained by the following equation for $C_{n_r(tail)}$:

$$C_{n_r(tail)} = -2\frac{l}{b}C_{n_\beta(tail)}$$

Inasmuch as the span of the present model is relatively small and the tail length large, the resulting value l/b for most of the vertical-tail configurations tested was approximately 1.0, whereas the value of l/b for the aspect ratio 6 model used in reference 9 was about 0.5. In addition, the values of $C_{n_\beta(tail)}$ for the present model were as

much as five times as large as those for the model of reference 9 partly because of the relatively smaller area and span on which the coefficients were based.

At no time during the flight tests with reduced directional stability were there any signs of oscillatory instability. The boundary for a lift coefficient of 0.7 with the flaps deflected, shown in figure 12, has been replotted in figure 15 together with the combinations of C_{n_β} and C_{l_β} with which flights were made to determine the effect of decreasing C_{n_β} by removing vertical-tail area. The combinations of C_{n_β} and C_{l_β} with which flights were made are on the stable side of the oscillatory stability boundary (fig. 15) which shows that the calculations are in agreement with the flight results. This boundary does not apply to the conditions where C_{n_β} was decreased by adding vertical-fin area forward of the center of gravity because the stability parameters used in the calculations were based on $C_{n_\beta(tail)}$ and therefore are not applicable to the boundary because many of the stability parameters $\left(\text{such as } C_{n_r}\right)$ would vary with the addition of the vertical fins forward.

CONCLUDING REMARKS

The results of power-off force and flight tests of a model equipped with a thin aspect ratio 3 unswept wing in the Langley free-flight tunnel are summarized as follows:

1. The static longitudinal stability characteristics of the model with flaps retracted were satisfactory. With the flaps deflected, the longitudinal stability decreased with increasing lift coefficient so that it was necessary to move the center of gravity forward to the leading edge of the mean aerodynamic chord to obtain stability at the stall.

2. Moving the horizontal tail upward increased the static longitudinal stability over the lift range but did not eliminate the variation in stability with lift coefficient for the flap-deflected configuration.

3. The dynamic longitudinal stability characteristics of the model were satisfactory with flaps retracted or deflected when satisfactory static stability was provided. When the static stability for the flap-deflected configuration was too low at the higher lift coefficients, an undesirable nosing-up tendency was present.

4. The model had high static directional stability over the entire lift range partly because a small amount of directional stability was obtained even with the vertical tail off.

5. The dynamic lateral stability characteristics of the model were satisfactory, and flights could be maintained easily with ailerons and rudder or ailerons alone at all lift coefficients up to the stall. The rolling motions, however, were faster and more difficult to control than those encountered with models of higher aspect ratio. At the stall, erratic rolling motions were encountered which were very difficult to control.

6. The flight characteristics were considered unsatisfactory when the directional-stability factor C_{n_β} was reduced below approximately 0.002 because large yaw angles were reached which caused difficulty in maintaining flight. More directional stability was required for the aspect ratio 3 model than for models of higher aspect ratio.

Langley Aeronautical Laboratory
    National Advisory Committee for Aeronautics
        Langley Field, Va.

Charles V Bennett
Charles V. Bennett
Aeronautical Engineer

James L Hassell Jr by CVB
James L. Hassell, Jr.
Aeronautical Research Scientist

Approved: *Thomas A. Harris.*
        Thomas A. Harris
    Chief of Stability Research Division

MLE

REFERENCES

1. McKinney, Marion O., Jr., and Shanks, Robert E.: Lateral Stability
     and Control Characteristics of a Free-Flying Model Having an
     Unswept Wing with an Aspect Ratio of 2. NACA TN No. 1658, 1948.

2. Shortal, Joseph A., and Osterhout, Clayton J.: Preliminary
     Stability and Control Tests in the NACA Free-Flight Wind Tunnel
     and Correlation with Full-Scale Flight Tests. NACA TN No. 810,
     1941.

3. Shortal, Joseph A., and Draper, John W.: Free-Flight-Tunnel
     Investigation of the Effect of the Fuselage Length and the
     Aspect Ratio and Size of the Vertical Tail on Lateral Stability
     and Control. NACA ARR No. 3D17, 1943.

4. Sternfield, Leonard: Effect of Product of Inertia on Lateral
     Stability. NACA TN No. 1193, 1947.

5. Zimmerman, Charles H.: An Analysis of Lateral Stability in Power-
     Off Flight with Charts for Use in Design. NACA Rep. No. 589,
     1937.

6. Toll, Thomas A., and Queijo, M. J.: Approximate Relations and
     Charts for Low-Speed Stability Derivatives of Swept Wings.
     NACA TN No. 1581, 1948.

7. Bamber, Millard J.: Effect of Some Present-Day Airplane Design
     Trends on Requirements for Lateral Stability. NACA TN No. 814,
     1941.

8. Drake, Hubert M.: The Effect of Lateral Area on the Lateral
     Stability and Control Characteristics of an Airplane as
     Determined by Tests of a Model in the Langley Free-Flight Tunnel.
     NACA ARR L5L05, 1946.

9. Drake, Hubert M.: Experimental Determination of the Effects of
     Directional Stability and Rotary Damping in Yaw on Lateral
     Stability and Control Characteristics. NACA TN No. 1104, 1946.

TABLE I

DIMENSIONAL AND MASS CHARACTERISTICS OF THE AIRPLANE MODEL

WITH ASPECT RATIO 3 WINGS

Wing:
    Area, sq ft 1.600
    Span, ft 2.192
    Aspect ratio 3.00
    Mean aerodynamic chord, ft 0.785
    Sweepback at 50 percent chord, deg 8
    Dihedral (relative to mean thickness line), deg 0
    Taper ratio (Tip chord/Root chord) 0.4
    Airfoil section . . . . Flat plate with tapered
                              leading and trailing edges

Vertical tail:
    Area, sq ft 0.215
    Height, ft 0.468
    Aspect ratio 1.02
    Sweepback of leading edge, deg 43
    Taper ratio (Tip chord/Root chord) 0.278
    Rudder area, sq ft 0.060
    Airfoil section . . . . Flat plate

Horizontal tail:
    Area, sq ft 0.295
    Span, ft 0.958
    Aspect ratio 3.140
    Sweepback of leading edge 22.5
    Taper ratio 0.444
    Elevator area 0.104
    Airfoil section . . . . Flat plate

Tail boom and dorsal fin area, sq ft 0.406
Fuselage fineness ratio 9:1
Fuselage length, ft 4.667
Over-all length, ft 5.992
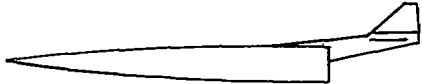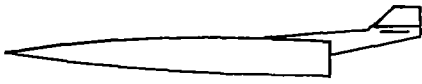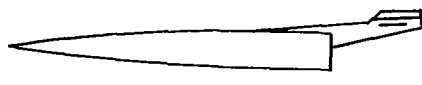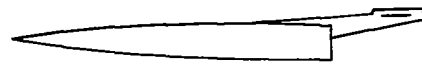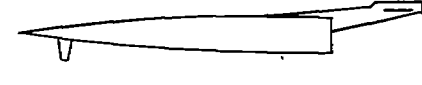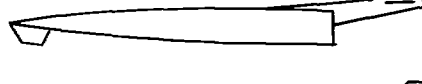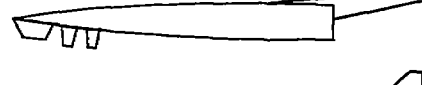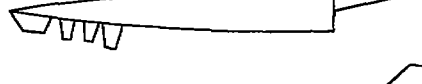
	Heavy loading		Light loading
Weight, lb	8.370	. . . . . .	6.845
Wing loading, lb/sq ft	5.230	. . . . . .	4.270
Moments of inertia, gm-in.^{2}:			
I_X	75,652	. . . . . .	41,325
I_Y	1,340,248	. . . . . .	971,769
I_Z	1,396,606	. . . . . .	987,186

TABLE II

VERTICAL TAIL CONFIGURATIONS TESTED AT
A LIFT COEFFICIENT OF 0.7 WHICH CORRESPONDS
TO ANGLE OF ATTACK OF 8°

CASE	C_{n_β}	C_{l_β}	C_{Y_β}	C_{n_r}	
I	0.0085	-0.0020	-0.015	-1.39	
II	0.0064	-0.0023	-0.014	-1.05	
III[A]	0.0019	-0.0016	-0.012	-0.51	
IV	0.0014	-0.0010	-0.010	-0.45	
V	-0.0005	-0.0010	-0.011	-0.53	
VI	0.0060	-0.0017	-0.016	-1.70	
VII	0.0044	-0.0019	-0.017	-1.87	
VIII	0.0023	-0.0016	-0.018	-2.02	
IX[A]	0.0018	-0.0017	-0.019	-2.11	
X[A]	0.0009	-0.0011	-0.020	-2.19	
XI	-0.0005	-0.0008	-0.021	-2.26	

[A]VALUES INTERPOLATED

TABLE III

CHARACTERISTICS OF AIRPLANE MODEL WITH ASPECT RATIO 3 WING USED IN CALCULATIONS OF THE

BOUNDARY OF ZERO DAMPING OF THE LATERAL OSCILLATIONS   (R = 0)

	$C_L = 0.6$; flaps up	$C_L = 0.7$; flaps down	$C_L = 1.0$; flaps down
W/S, lb/sq ft	4.27	4.27	4.27
b, ft	2.192	2.192	2.192
ρ, slugs/cu ft	0.002378	0.002378	0.002378
V, ft/sec	77.7	71.8	61.0
μ	25.619	25.619	25.619
k_X, ft	0.304	0.304	0.304
k_Z, ft	1.486	1.486	1.486
C_{l_p}, per radian	$-0.25 - 0.0247C_{n_\beta(tail)}$	$-0.27 - 0.0478C_{n_\beta(tail)}$	$-0.25 - 0.018C_{n_\beta(tail)}$
C_{l_r}, per radian	$0.15 + 0.212C_{n_\beta(tail)}$	$0.175 + 0.295C_{n_\beta(tail)}$	$0.25 + 0.1812C_{n_\beta(tail)}$
C_{n_p}, per radian	$0.055 + 0.212C_{n_\beta(tail)}$	$-0.032 + 0.295C_{n_\beta(tail)}$	$-0.068 + 0.1812C_{n_\beta(tail)}$
C_{n_r}, per radian	$-0.015 - 1.82C_{n_\beta(tail)}$	$-0.072 + 1.82C_{n_\beta(tail)}$	$-0.087 - 1.82C_{n_\beta(tail)}$
C_{Y_p}	0	0	0
C_{Y_r}	0	0	0
C_{Y_β}, per radian	$-0.460 - 1.10C_{n_\beta(tail)}$	$-0.573 - 1.10C_{n_\beta(tail)}$	$-0.515 - 1.10C_{n_\beta(tail)}$
$C_{n_\beta(tail off)}$, per radian	0.000	0.000	0.000
γ, deg	-17.5	-20.0	-18.6
α, deg	10	7.5	11.0
η, deg	7	4.5	8
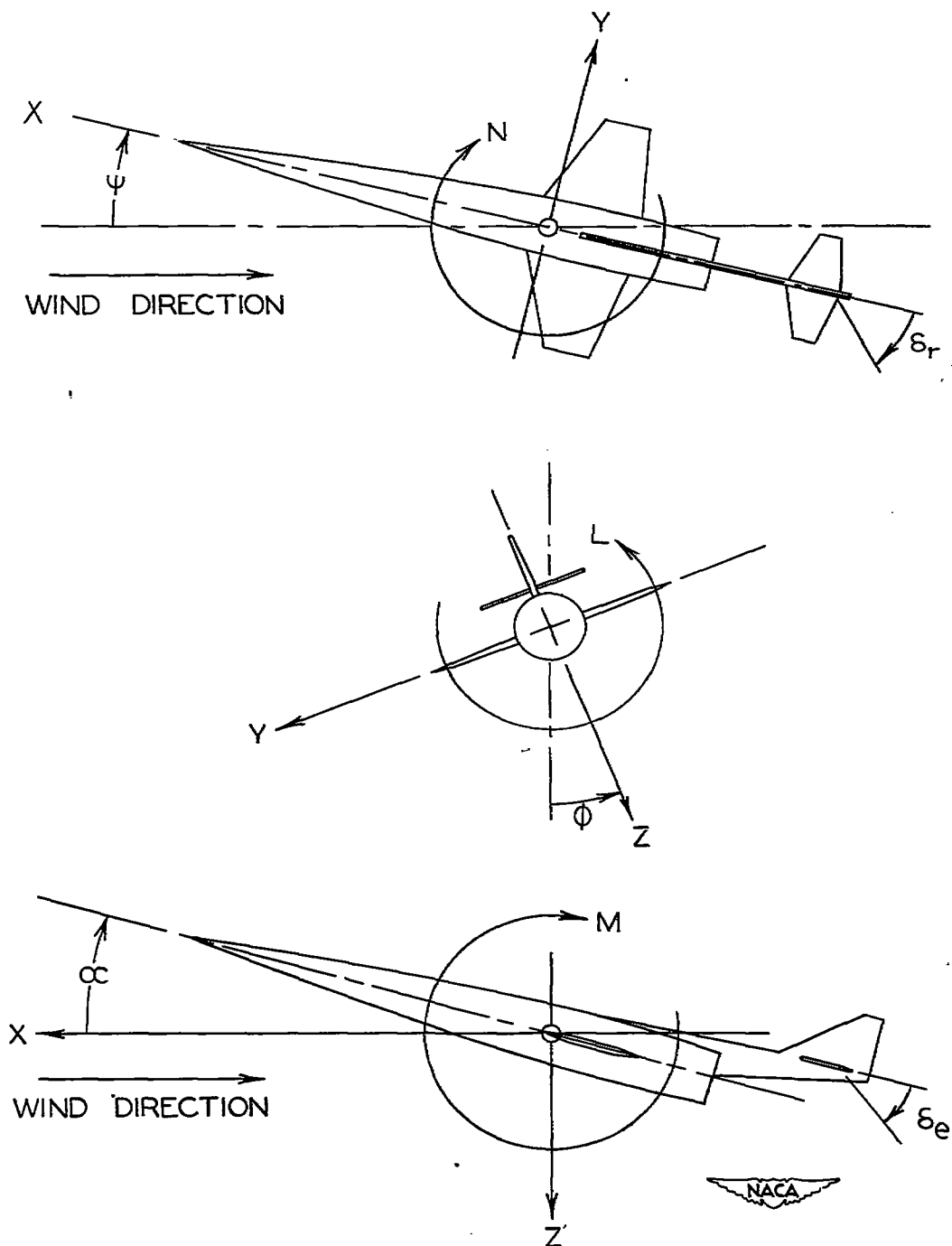
Figure 1.- The stability system of axes. Arrows indicate positive directions of moments, forces, and control-surface deflections. This system of axes is defined as an orthogonal system having the origin at the center of gravity and in which the Z-axis is in the plane of symmetry and perpendicular to the relative wind, the X-axis is in the plane of symmetry and perpendicular to the Z-axis, and the Y-axis is perpendicular to the plane of symmetry.
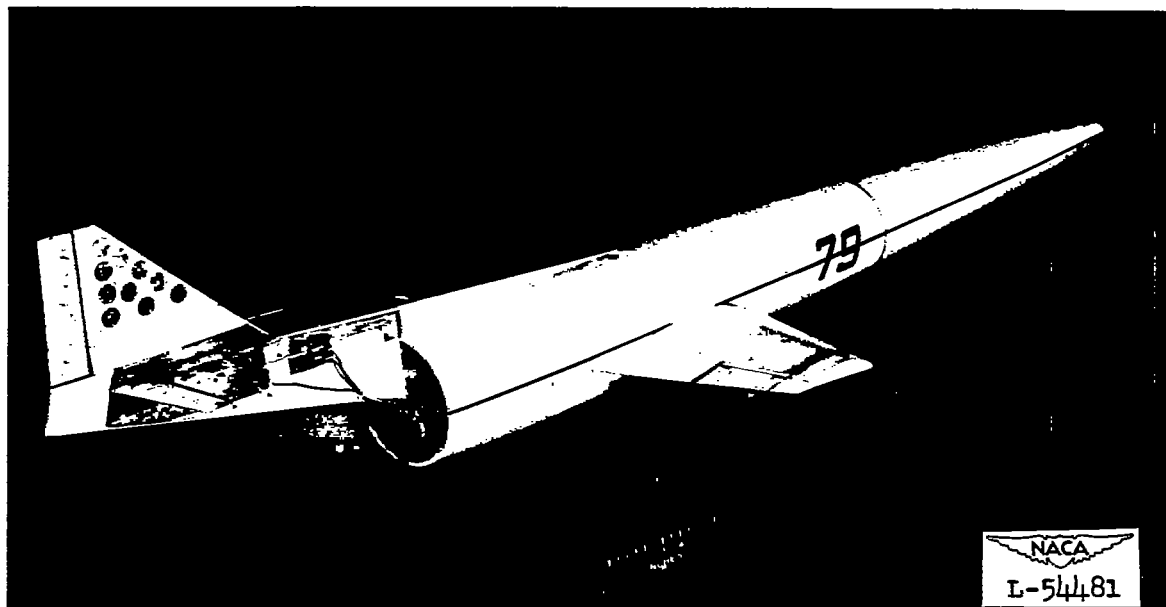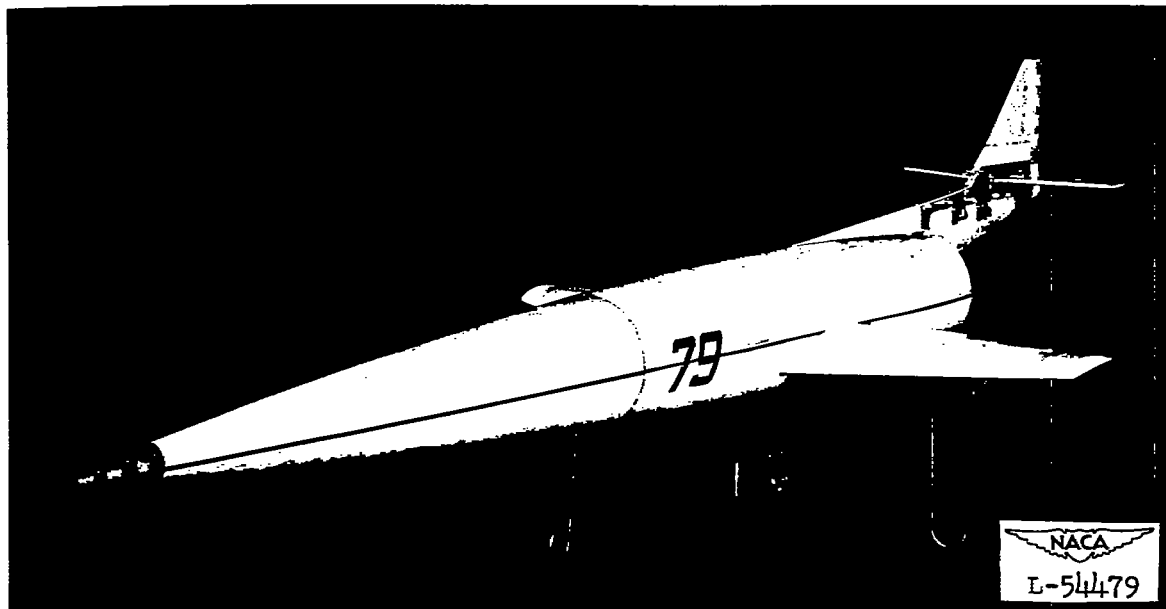
Figure 2.- Photographs of the model used in the tests. (Model was equipped with a double-wedge section instead of the cambered section as shown.)

MAC

0.30 C SPLIT FLAPS

AILERON 0.25 C

50" 5.0"

A

A

0.15 C NOSE FLAP

2.37"

5.61"

FLAP DOWN CONFIGURATION

0.15C

0.30C

30°

0.45C

60°

SECTION A-A

23.90"

CG AT .10c̄

C.P.

71.9"

26.26"

NACA
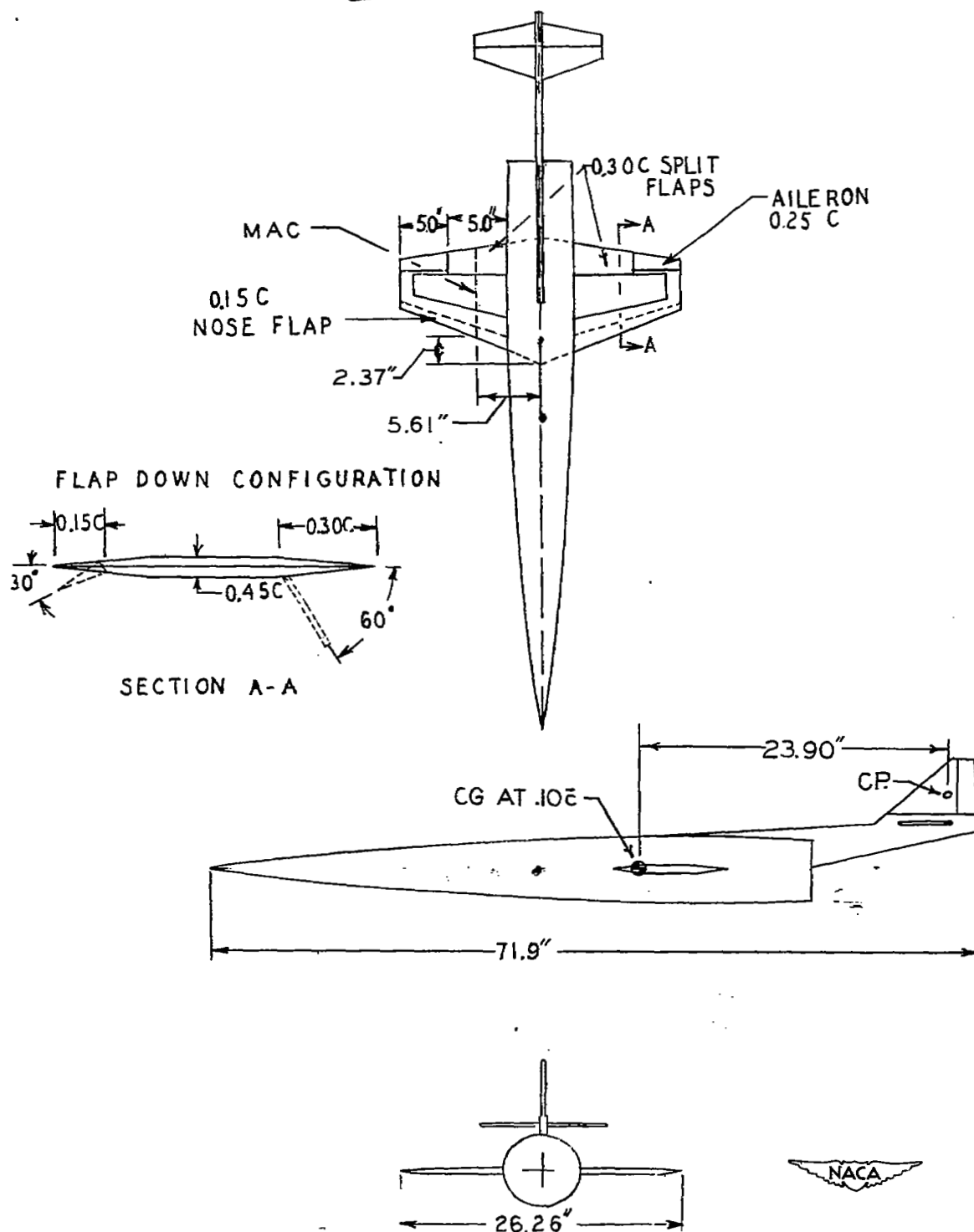
Figure 3.- Three-view sketch of test model.
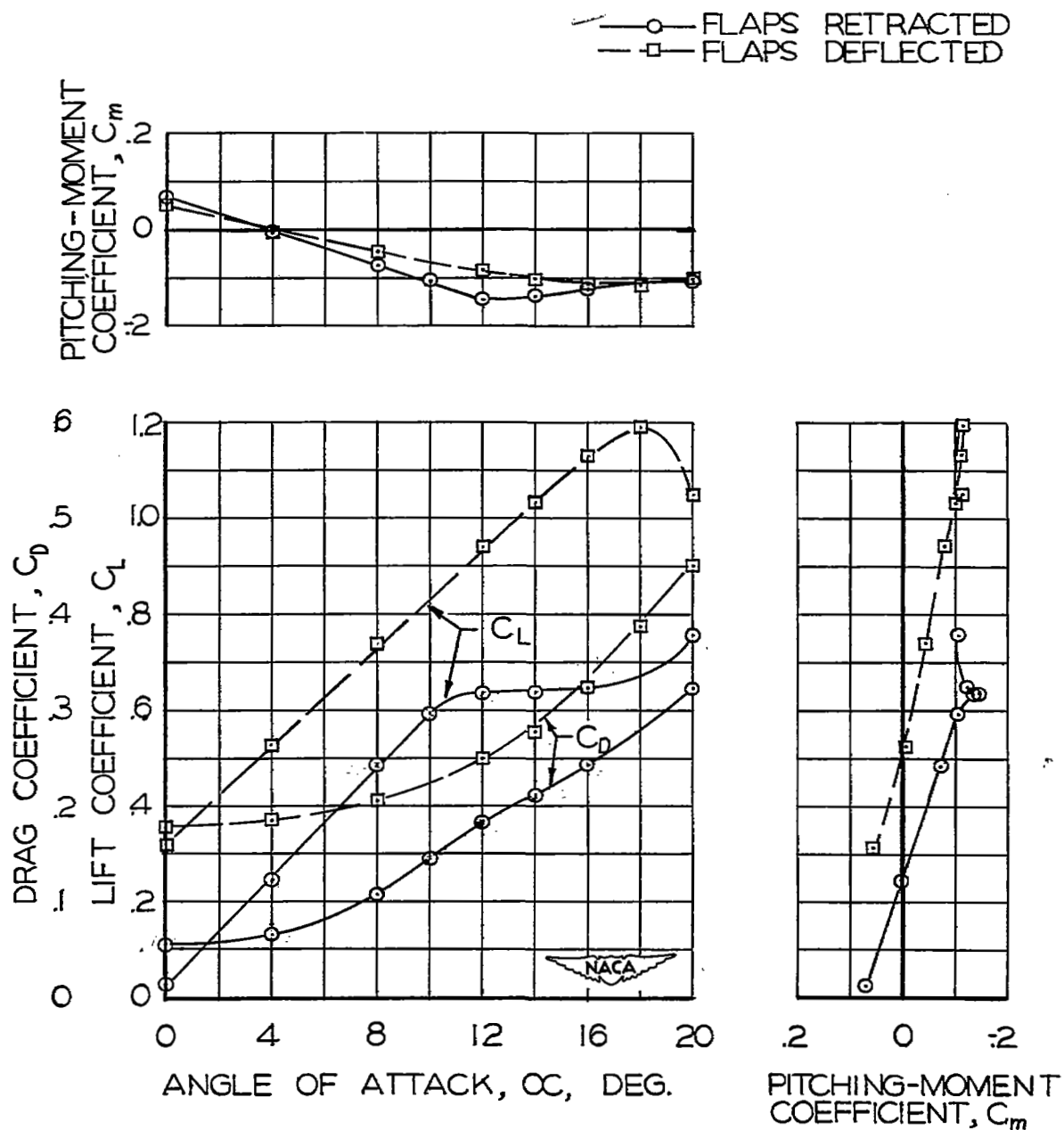
Figure 4.- Effect of flap deflection on the lift, drag, and pitching-moment characteristics of the test model. Center of gravity at leading edge M.A.C.; $i_t = 0$.

Figure 5.- Effect of horizontal-tail incidence on the lift, drag, and pitching-moment characteristics of the test model with flaps retracted. Center of gravity at leading edge M.A.C.
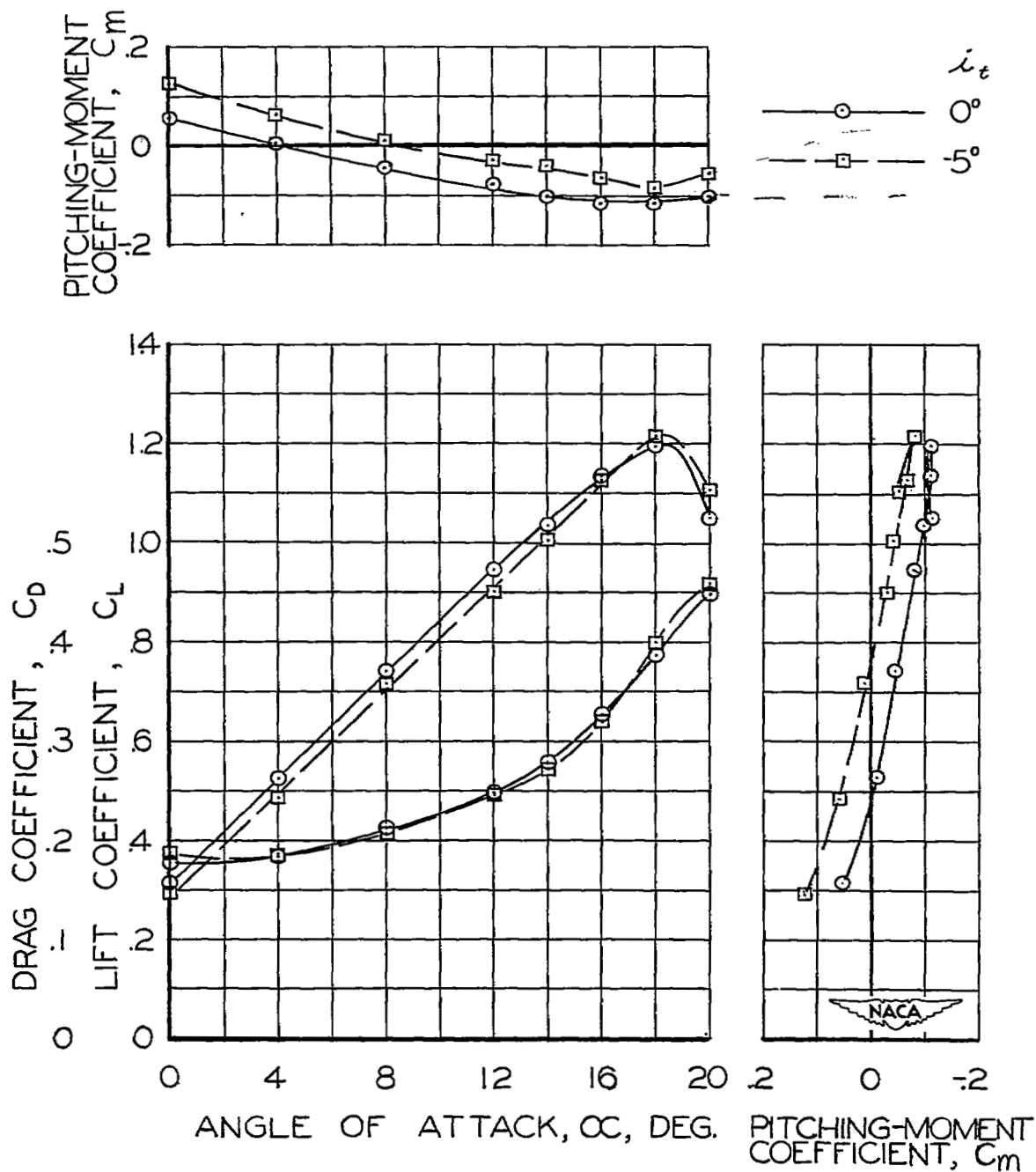
Figure 6.- Effect of horizontal-tail incidence on the lift, drag, and pitching-moment characteristics of the test model with flaps deflected and with the center of gravity at leading edge M.A.C.
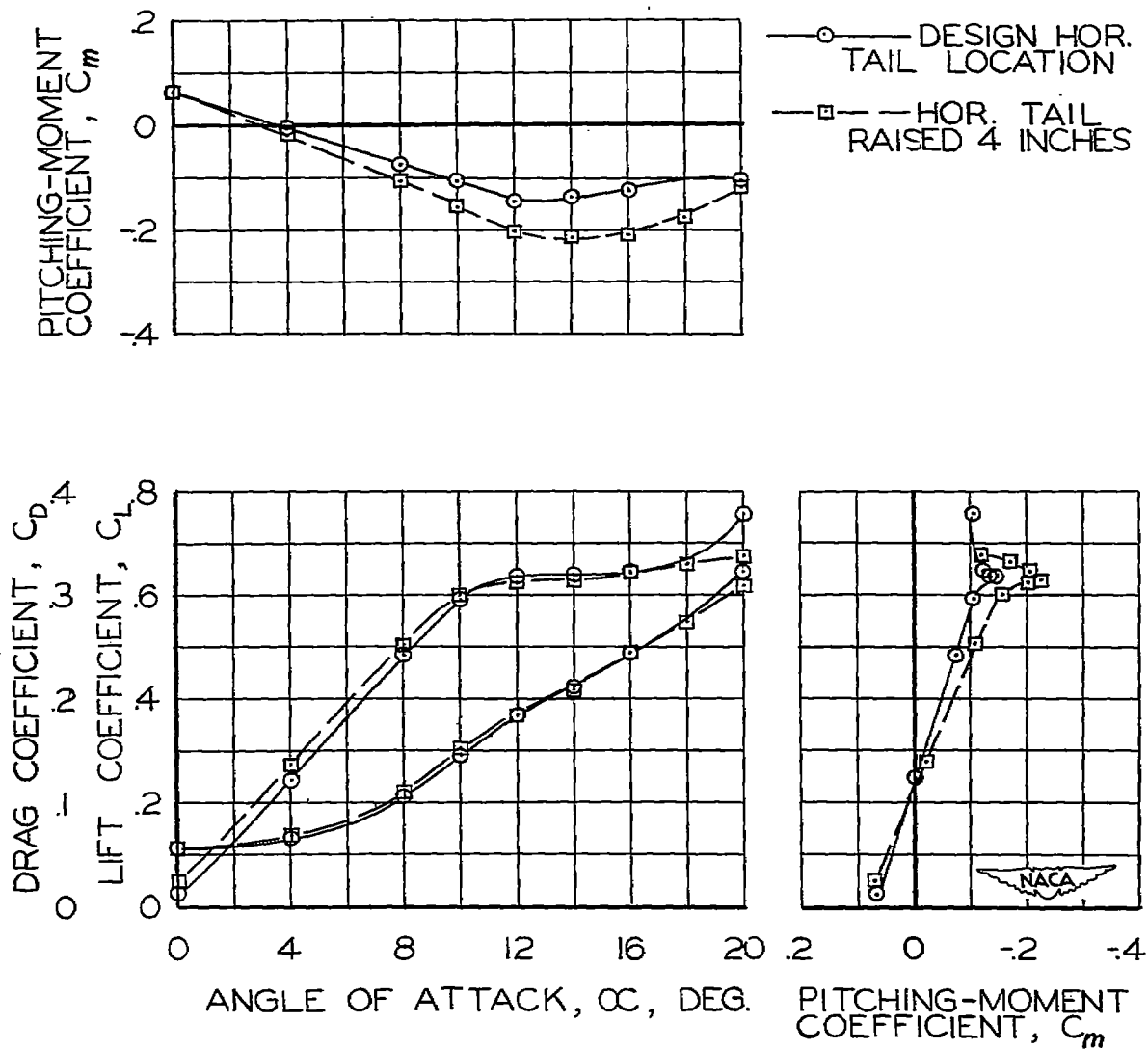
Figure 7.- Effect of horizontal-tail location on the lift, drag, and pitching-moment characteristics of the test model with flaps retracted. Center of gravity at leading edge M.A.C.; $i_t = 0$.

CONFIDENTIAL
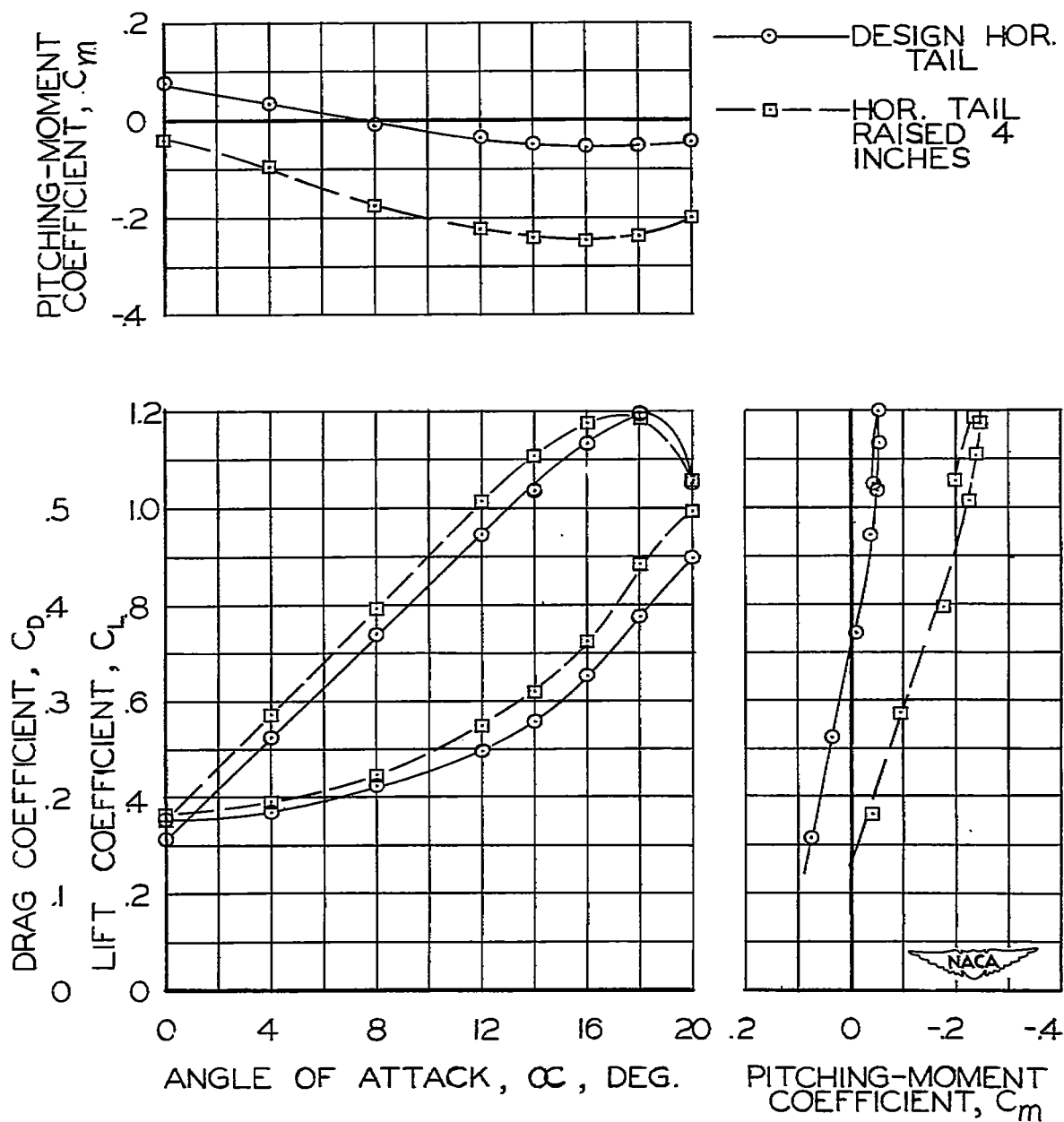
Figure 8.- Effect of horizontal-tail location on the lift, drag, and pitching-moment characteristics of the test model with flaps deflected. Center of gravity at 0.05 M.A.C.; $i_t = 0$.

CONFIDENTIAL
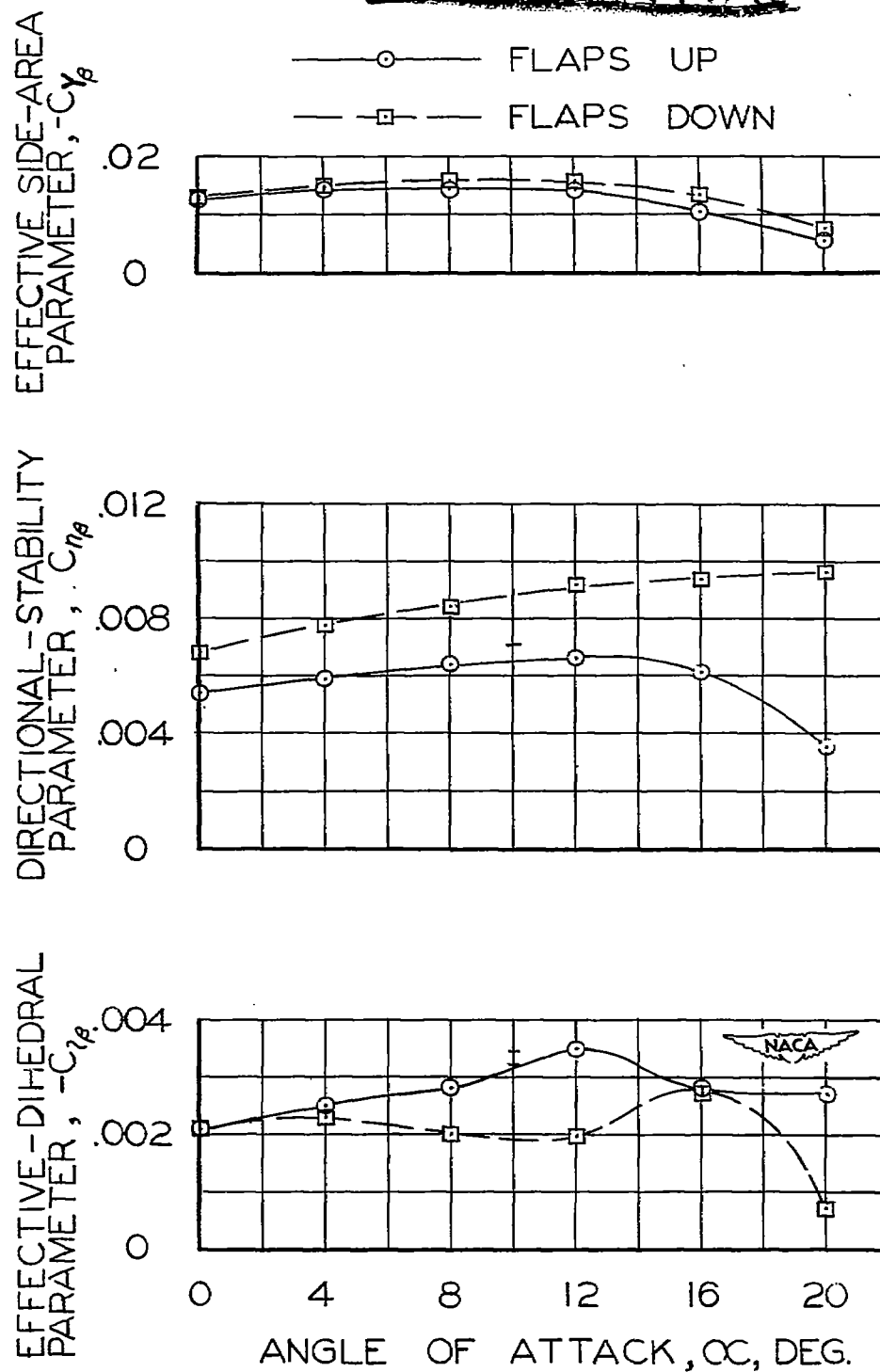
Figure 9.- Effect of flap deflection on the static lateral stability characteristics of the test model. Center of gravity at 0.10 M.A.C.; $i_t = 0$.
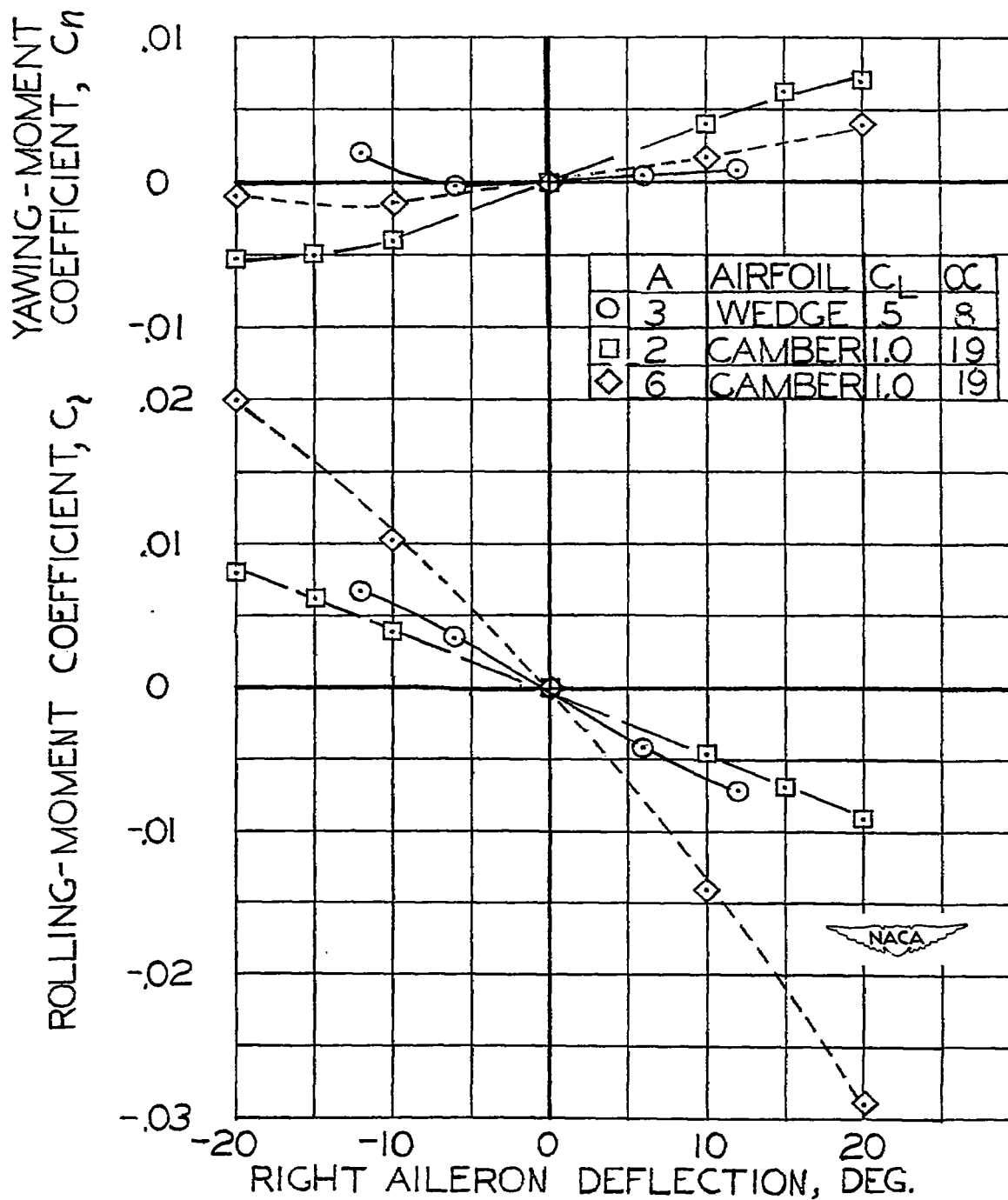
Figure 10.- Aileron rolling and yawing effectiveness for the aspect
ratio 3 wing compared to those for A = 2 and A = 6 wings of
reference 1.

AIRFOIL		SOURCE
—O—	SHARP NOSE	TEST
—□—	ROUND NOSE	TEST
------	ROUND NOSE	CALC.
— — —	SHARP NOSE	CALC.

$$C_{n_p} = -\left(\frac{C_L - C_D \alpha}{8}\right) \text{REF. 5}$$

ANGLE OF ATTACK, α, DEG.

NACA
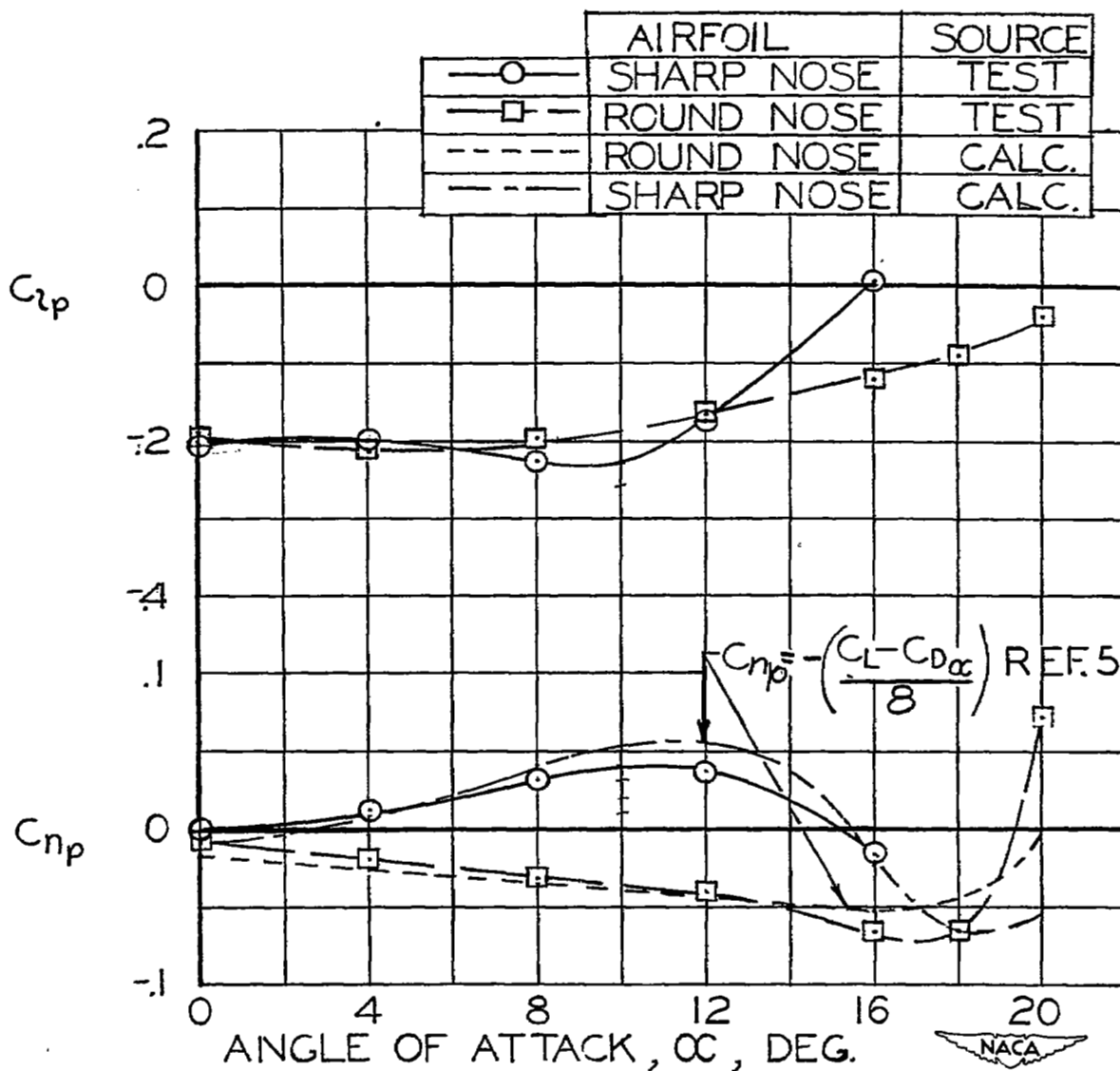
Figure 11.- Comparison of C_{l_p} and C_{n_p} for the sharp-nose test wing and for a round-nose wing of identical plan form.

STABLE

UNSTABLE

FLAPS EXTENDED
$C_L = 0.7$

FLAPS EXTENDED
$C_L = 1.0$

FLAPS RETRACTED
$C_L = 0.6$

DIRECTIONAL STABILITY PARAMETER, C_{n_β}

EFFECTIVE DIHEDRAL PARAMETER, $-C_{l_\beta}$
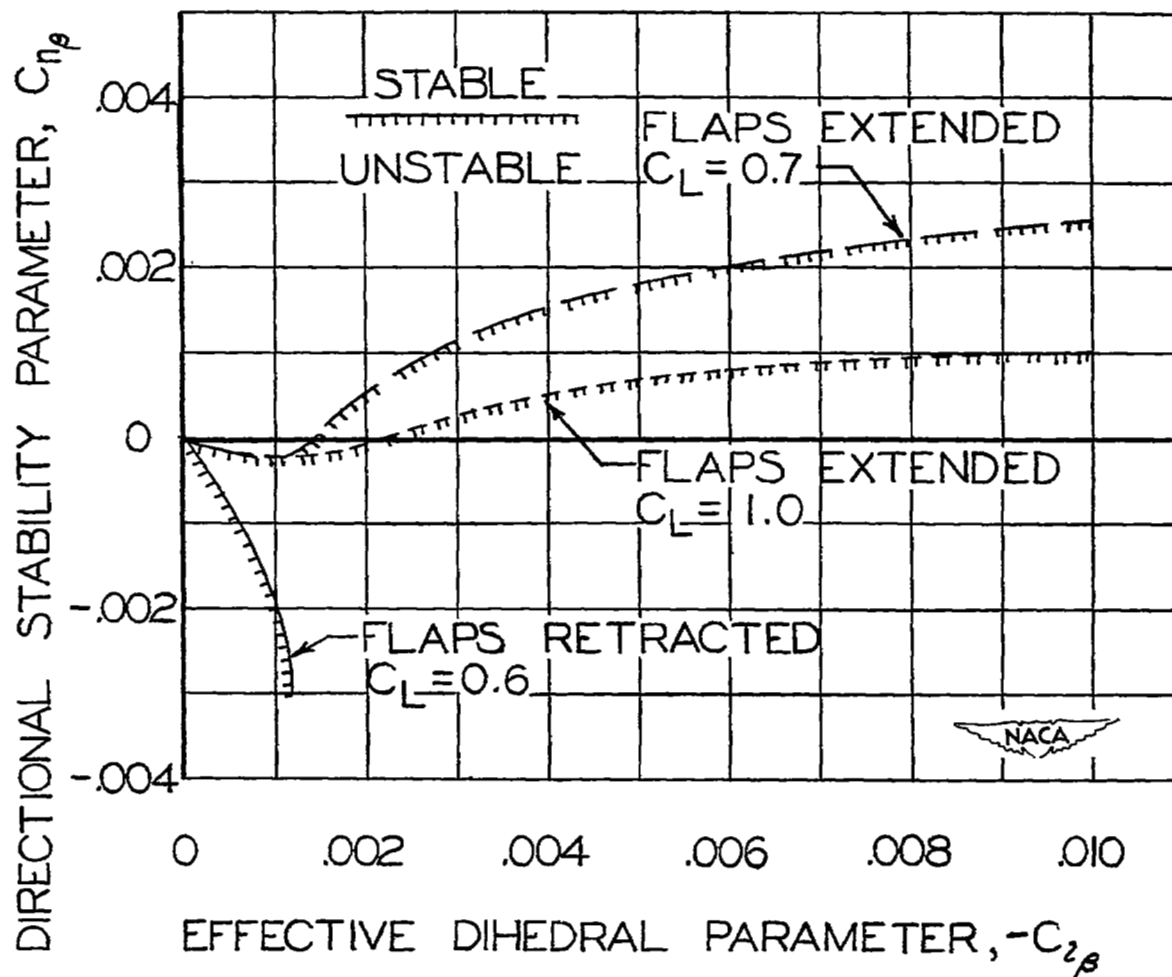
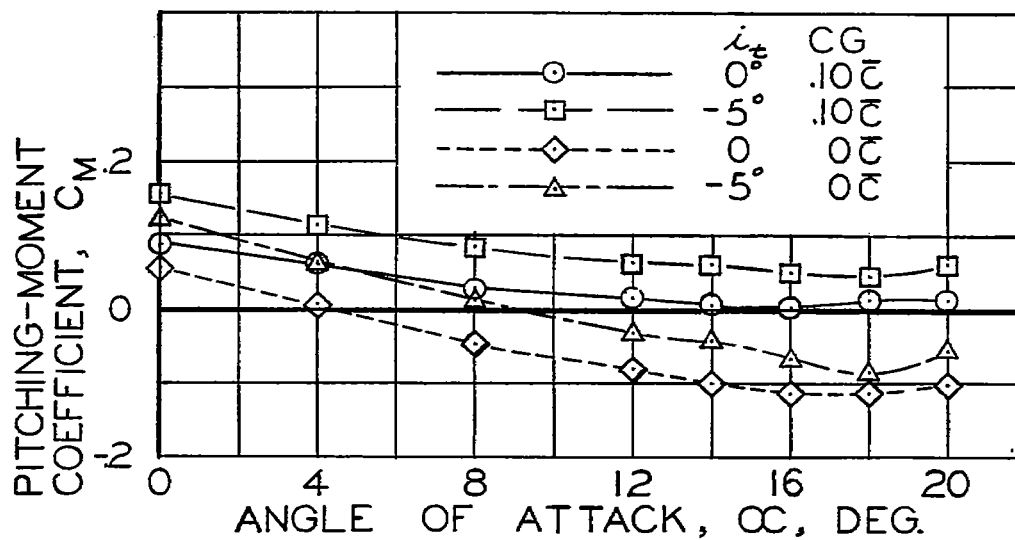Figure 12.- Calculated oscillatory-stability boundaries for the test
model. (See table III for conditions.)
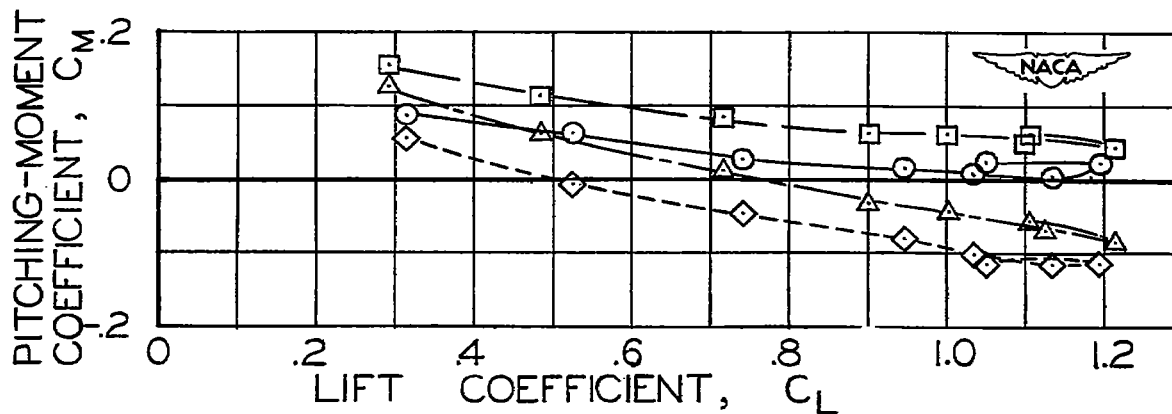
Figure 13.- Effect of tail incidence on the pitching-moment characteristics of the test model with flaps deflected for center-of-gravity locations of 0 and 0.10 M.A.C.
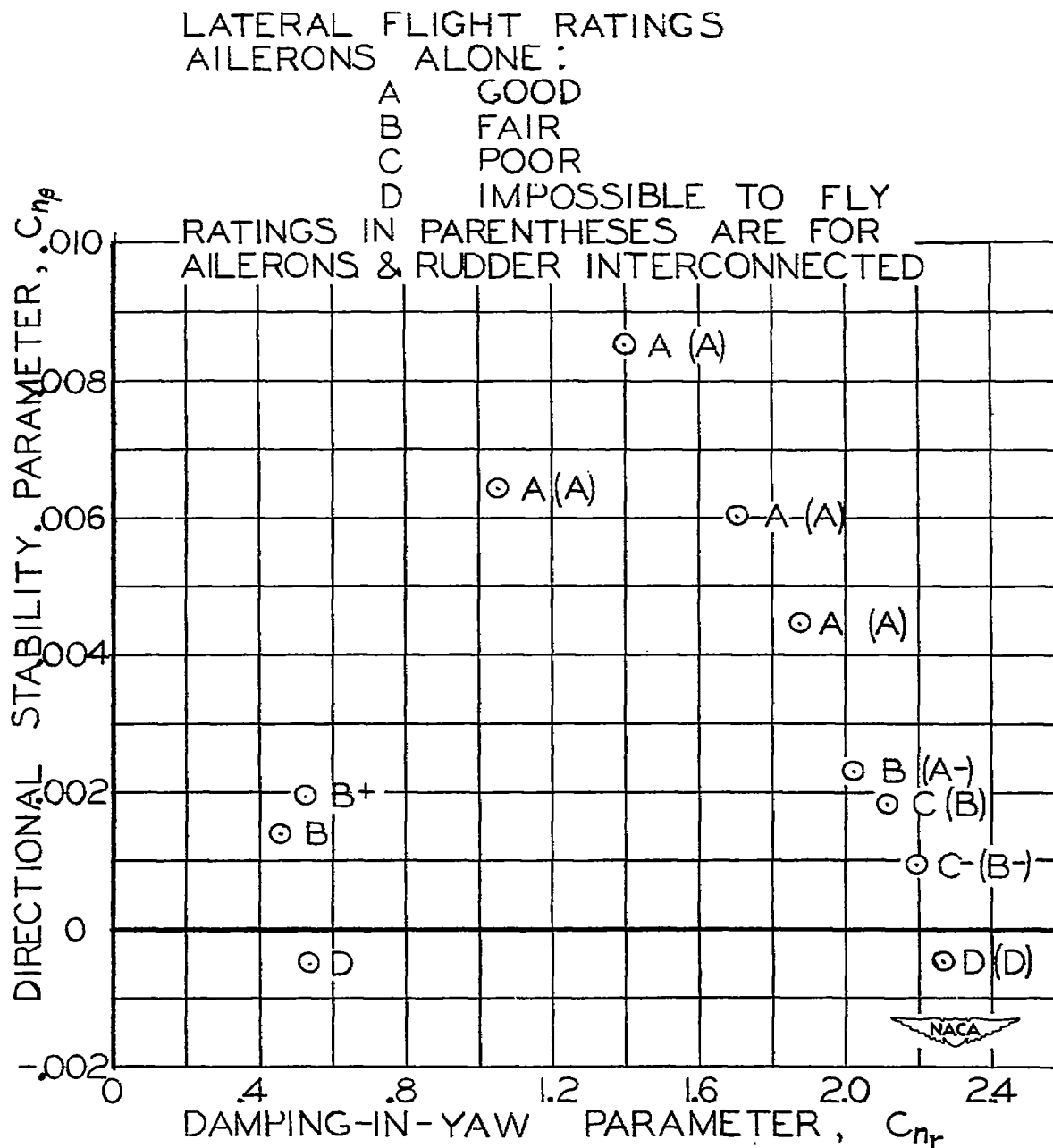
CONFIDENTIAL

LATERAL FLIGHT RATINGS
AILERONS ALONE :

A   GOOD
B   FAIR
C   POOR
D   IMPOSSIBLE TO FLY

RATINGS IN PARENTHESES ARE FOR
AILERONS & RUDDER INTERCONNECTED

Figure 14.- Summary of the lateral flying characteristics of the test
model as were observed by the pilot during flights in which the
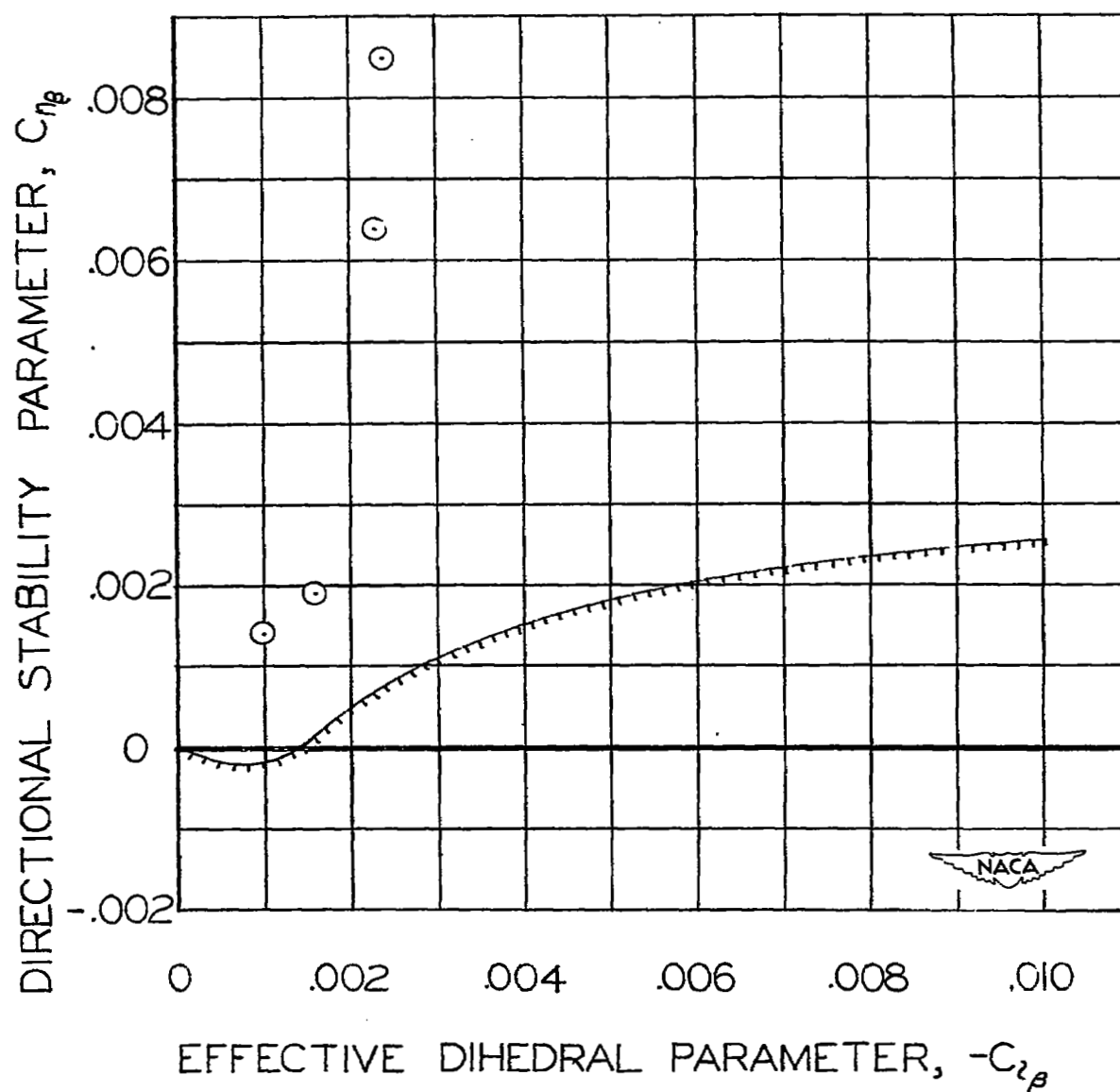directional stability was varied.

CONFIDENTIAL

Figure 15.- Flap extended lateral-stability boundary for a lift coefficient of 0.7. Symbols represent combinations of C_{n_β} and C_{l_β} that were flown.

CONFIDENTIAL

INDEX

ABSTRACT

The results of power-off force tests and flight tests of a model with a thin unswept low-aspect-ratio wing are presented. The tests were made with the flaps retracted and deflected and the effects on the lateral flight characteristics of decreasing directional stability were noted.

CONFIDENTIAL